Aerodynamic Analysis and Optimization of a Coaxial Helicopter Fuselage

Lukas Rottmann
Deutsches Zentrum für Luft- und Raumfahrt e.V. Braunschweig, Lilienthalplatz 7, 38106 Braunschweig, lukas.rottmann@dlr.de

The flight dynamics and flight envelope of coaxial ultralight helicopter CoAX 2D were investigated in the national LuFo project CURoT (Coaxial Ultralight Rotorcraft Technology). For this purpose, series of flight tests was carried out. This paper presents the computation of the fuselage aerodynamics of the CoAX 2D. The actual state of the existing configuration for different flight conditions is investigated. In addition, optimization potentials of the cell are examined. Finally, the influence of an optimized chassis was analysed and a reduction of the drag could be shown.

Introduction:

The main difference between a classic helicopter configuration with main and tail rotor to a coaxial helicopter is that the coaxial helicopter does not require a tail rotor. The rotor torque is balanced by the arrangement of counter-rotating main rotors. This saves the power required for the tail rotor. The omission of the tail rotor allows a compact and very light construction which makes the coaxial helicopter also interesting for urban operations [1]. From the pilot's point of view, the coaxial helicopter offers advantages in terms of better handling qualities. For example, only little yaw control is required when the collective pitch of the main rotor changes [2].
The company edm-aerotec in Geisleden, Germany took advantage of these benefits to develop the CoAX 2D, shown in Figure 1, and had a successful maiden flight in 2015 [3]. In the context of the Lufo project CURoT (Coaxial Ultralight Rotorcraft Technology), the CoAX 2D was used in a cooperation between edm-aerotec, the Technical University Munich and DLR to investigate aeromechanical and aerodynamic phenomena that occur especially for coaxial helicopter configurations. For this purpose, edm-aerotec performed measurement flights with the CoAX 2D. Sensors were available to determine the GPS position, acceleration and roll, pitch and yaw angles. A nose boom measured the true air speed. In addition to the measurements taken to determine the flight condition, the pilot's control forces and the control input were also recorded. For the analysis of the aerodynamic forces at the stabilizers, the structural deflection and the torsion moments at the tail boom were measured by means of strain gauges. Two rotating measurement units for the upper and lower main rotor blades were mounted to record the flap and lead-lag moments as well as the teeter angle of the individual blades [4].
To analysis the flight tests, a analysis model using the comprehensive code Camrad II was developed by the Technical University of Munich and validated with the flight measurement data [5]. Based on these results, the DLR Institute of Aerodynamics and Flow Technology contributes its competences in the field of fuselage aerodynamics to this Lufo project and investigated the fuselage cell of the CoAX 2D by using the flow solver TAU developed by DLR. Further optimization potential is proposed.

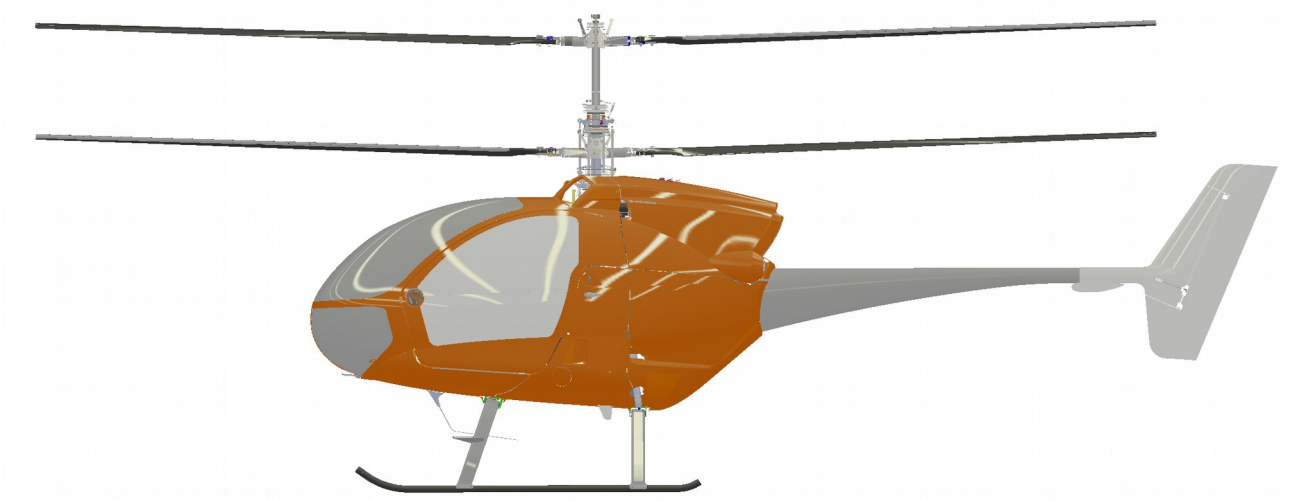

Figure 1:side view from CoAX 2D

CoAX 2D:
The CoAX 2D coaxial helicopter is an ultra-light helicopter with a maximum take-off mass of 450kg and was developed by edm-aerotec in Geisleden. It has a 84 kW piston engine and offers spaceseating for a pilot and a copilot. All parts from the CoAX 2D with the exception of the engine and the cell, are produced in Geisleden [6]. The main rotor blades of the upper and lower main rotor plane are identical and are rectangular rotor blades with a twist. The rotation direction of the lower rotor is clockwise while the upper rotor rotates counterclockwise.
The fuselage of the CoAX 2D is symmetrical. The fuselage cell is tilted by 4° to the rotorshaft. Figure 1 shows on the one hand the angle of the fuselage compared to the rotor shaft and that on the other hand the landing skids and rotor shaft are at perpendicular to each other.

Methodology:
The DLR flow solver TAU was used to analyse the CoAX 2D fuselage. The TAU-code solves the compressible Reynolds-averaged Navier-Stokes equations on hybrid unstructured meshes around complex geometries. The spatial discretization the fluxes are of second order accuracy. Different turbulence models are available to conclude the system of equations. In order to accelerate the simulation, the TAU code provides a multi-grid procedure [7]. For the simulation of the rotor downwash of the CoAX 2D, the Actuator Disc approach in the TAU code was chosen. The Actuator Disc represents a finite plane with zero thickness in the computational mesh. Using an input of an external force for the Actuator Disc, the Actuator Disc generates a discontinuous jump of the flow across the rotor plane [8]. The input for the Actuator Disc comes from the comrehensive rotor code Camrad II. The model of the CoAX 2D in Camrad II was realized by the Technical University of Munich. Camarad II is a comrehensive rotor code for the simulation of rotorcraft. Multi-body-dynamics, nonlinear finite element, structural dynamics and rotorcraft aerodynamics as well as trim procedures are considered [9].

Case Studies:
The analysis of the CoAX 2D fuselage cell divided into three steps. In the first step, fuselage polars are simulated by varying the angle of attack and yaw angle at constant airspeed and without rotor downwash. In the second part the flow of the CoAX 2D is investigated for which the rotor downwash modeled using the Actuator Disc. Each Actuator Disc input corresponds to a trimmed flight condition. In addition to different flight speeds, climb and descent speeds are also considered. Concepts for optimizing the fuselage are then developed on the basis of the previous results. For the first and second part a hybrid mesh with 7.8 mio. points was created. The underlying CAD geometry of CoAX 2D simplified. The rotor head is replaced by a simplified geometry. In addition, all ducts within the fuselage are neglected and all gaps were closed. All attachments such as antennas were also omitted. Also the mounting of the landing gear to the fuselage is simplified. For the optimization of the landing gear new meshes are created.

Fuselage polar:
For the determination of the fuselage polar without influence of the rotor downwash, a polar angle of attack of 18° to -18° is simulated for a cruising velocity of 33.3 m/s for the yaw angles of 0°, 2° and 4°. Due to the symmetry of the fuselage, no negative yaw angles are simulated. A convergence of at least six orders of magnitude is ensured for all simulations. Figure 2 shows the drag coefficient over the angle of attack of the fuselage for different yaw angles. Positive angles of attack denote a pitch up, negative angles denote a pitch down. The CoAX 2D has its minimum drag at minus eight degrees angle of attack even for different yaw angles, where the airframe is aligned to the flow at minus four degrees. With increasing and decreasing angle of attack, the drag of the fuselage also increases.

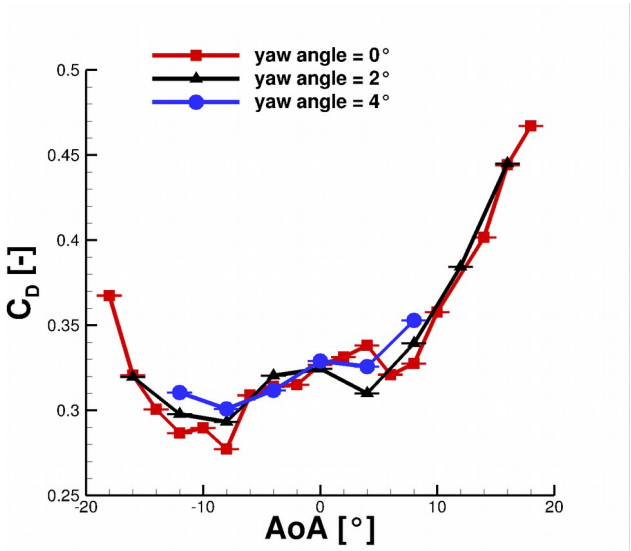

Figure 2: drag coefficient over angle of attack

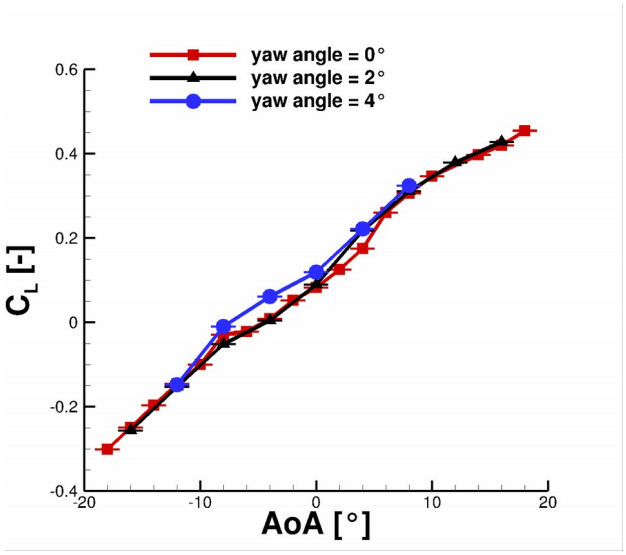

Figure 3: lift coefficient over angle of attack

The lift coefficient of the CoAX 2D is sketched in Figure 3. The simulation show a linear behavior with respect to the lift coefficient even for different yaw angles, no collapse of the lift coefficient are detected in range ±18°.
With regard to the pitching moment, Figure 4 shows that the CoAX 2D has a consistently slightly negative pitch torque coefficient in the range between ±5°.

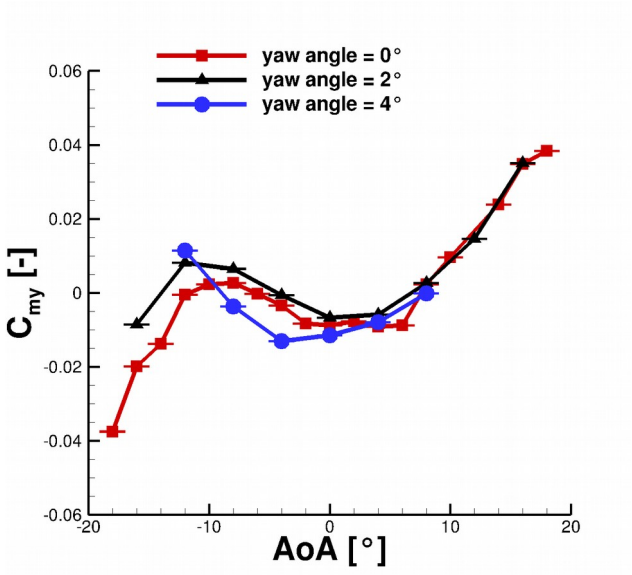

Figure 4:pitching moment coefficient over angle of attack

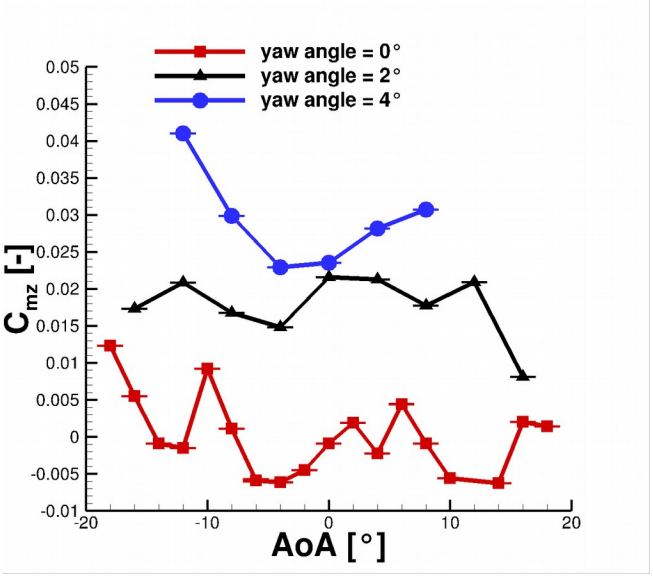

Figure 5:yawing moment coefficient over angle of attack

A negative pitching moment leads to a nose down motion. The moment reference point is located on the rotor axis of the CoAX 2D. As the angle of attack decreases, a negative pitching moment is increasingly detected and a positive pitching moment is detected for increasing angles of attack. As the yaw angle increases, there is also an raise in the yaw moment, as seen in Figure 5.

Flight polar:

In order to investigate the flow of the CoAX 2D more closely, the second section varied the angle of attack and the airspeed. In order to increase the accuracy of the simulation, the rotor downwash is modeled using an Actuator Disc. The input data for the Actuator Disc as well as the angle of attack of the fuselage cell are provided by the Camrad II model of the CoAX 2D. Each Actuator Disc input corresponds to a trimmed flight condition. The flight conditions calculated in Camrad II are based on the flight tests performed by edm-aerotec [3,4]. In addition to various forward flight speeds, climb and descent flights are also calculated.

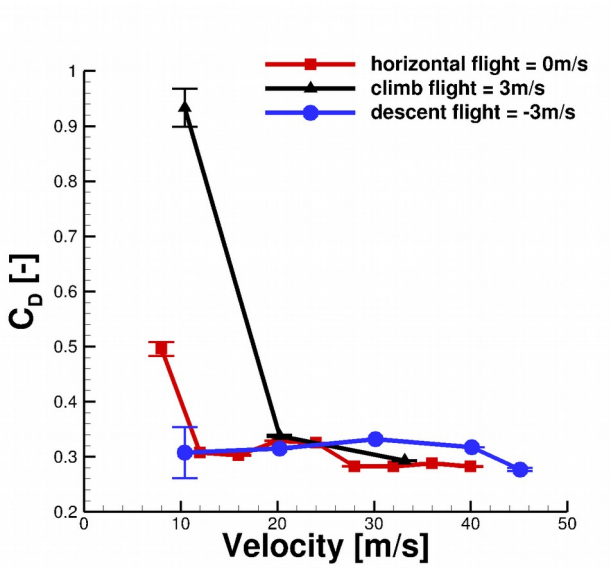

Figure 6: drag coefficient over velocity

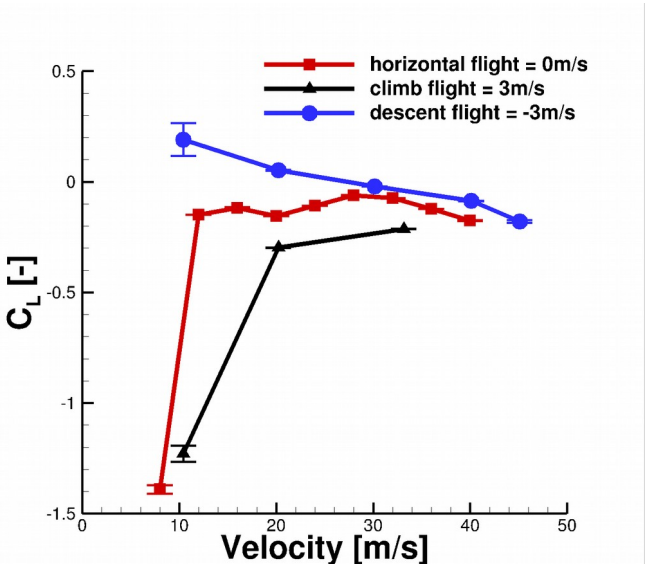

Figure 7: lift coefficient over velocity

Figure 6 shows the drag coefficient in the aerodynamic coordinate system over speed. It is shown that the coefficient of drag moves in a range from 20 m/s to 45 m/s also for different climb and sink rates in a similar range.
Figure 7 shows the lift coefficient over velocity. Positive lift coefficients counteract the weight of the helicopter. In the range between 20 m/s and 45 m/s, no major changes in the lift coefficient are detected too. Whereas the lift coefficient changes between descent flight, horizonal flight and climb flight. This shows that the fuselage generates additional lift during descent and thus relieves the main rotors. A comparison of the flight polars and fuselage polars for a speed of 32 m/s shows that both, the lift coefficient and the drag coefficient, are reduced by the rotor downwash.
Finally, it is clarified why the CoAX 2D shows a drastic increase of the drag coefficient on the one hand and a decrease of the lift coefficient on the other hand for speeds below < 20 m/s. Figures 8 and 9 show the dimensionless eddy viscosity for two different speeds and similar drag coefficient. The eddy viscosity is an artifical viscosity added to the RANS equations by the turbulence model and may be used as an indication for regions of seperated flows. Figure 8 shows a much larger separation area behind the fuselage then the slower flight in Figure 9. Since the drag increases proportionally with speed, both cases have a similar value for the dimensionless drag coefficient.

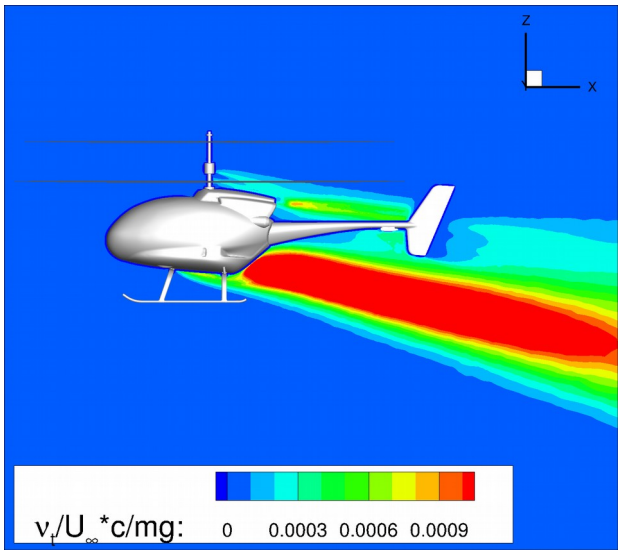

Figure 8: Horizontal flight, velocity = 32 m/s

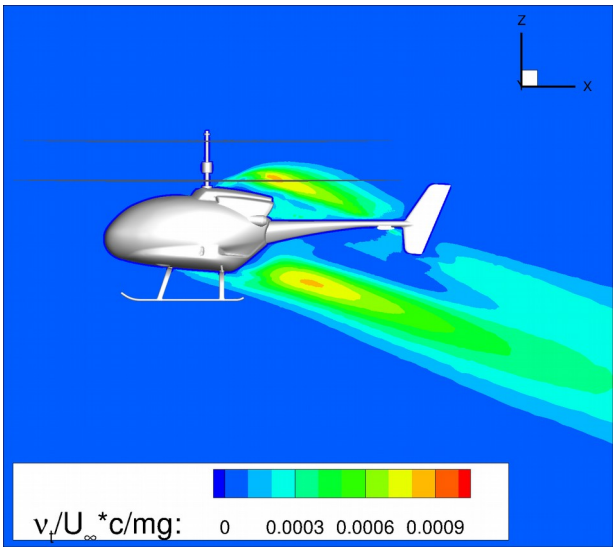

Figure 9 : Horizontal flight, velocity = 12 m/s

In order to find an explanation for the difference in drag coefficent between climb an descent flight, the dimensionless eddy viscosity is also shown in Figures 10 and 11. Figure 10 shows the eddy viscosity for a climb speed of 3 m/s and Figure 11 for descend speed of -3 m/s with a horizontal speed of 10 m/s. It seen that especially the climb has a much larger separation area than the descent. During climb the local eddy viscosity is smaller, but a strong separation of the horizontal stabilizer is observed.

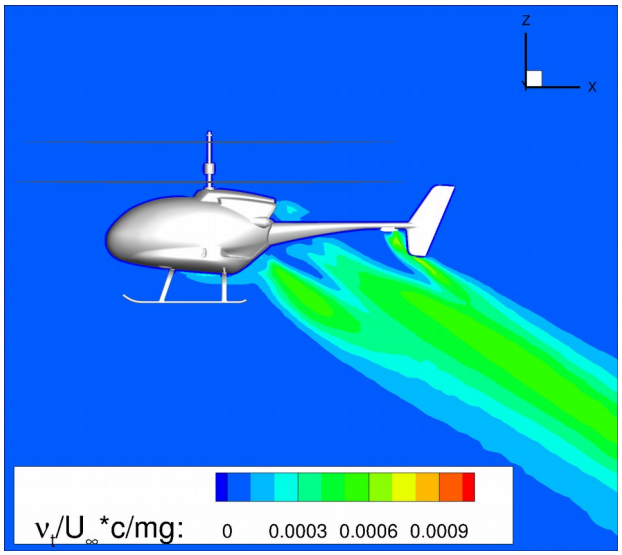

Figure 10: Climb flight, velocity = 10 m/s

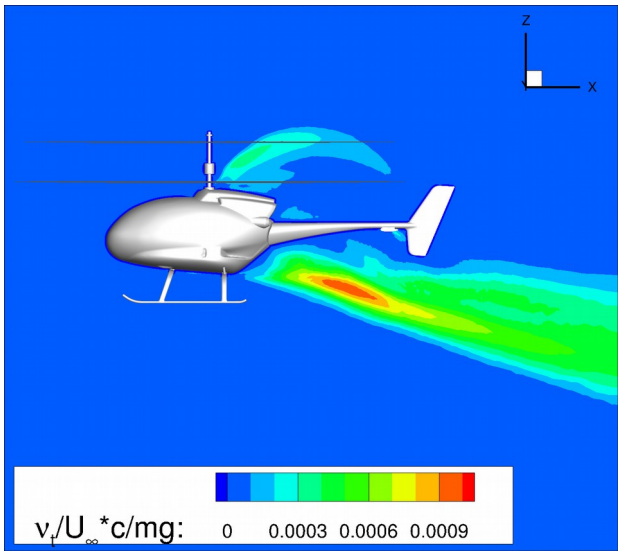

Figure 11: Descent flight, velocity = 10 m/s

The separation at the horizontal stabilizer is noticed in the pitching moment coefficient in Figure 12, where the pitching moment coefficient has its highest value both for horizontal flight at 8 m/s and for climb flight at 10 m/s. For descent flight there is no separation of the horizontal stabilizer at 10 m/s speed. The higher the speed, the smaller the influence of the main rotors and the pitch moment coefficient decreases. A comparison of the yawing moments in Figure 13 shows an increase from descent to climb.

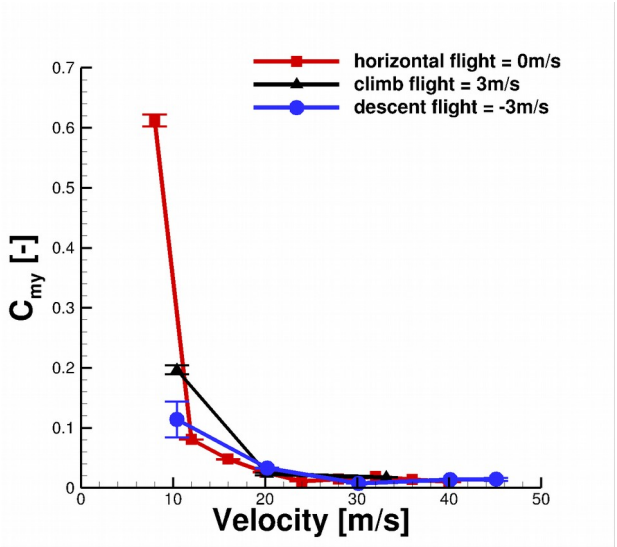

Figure 12: Pitching moment over Velocity

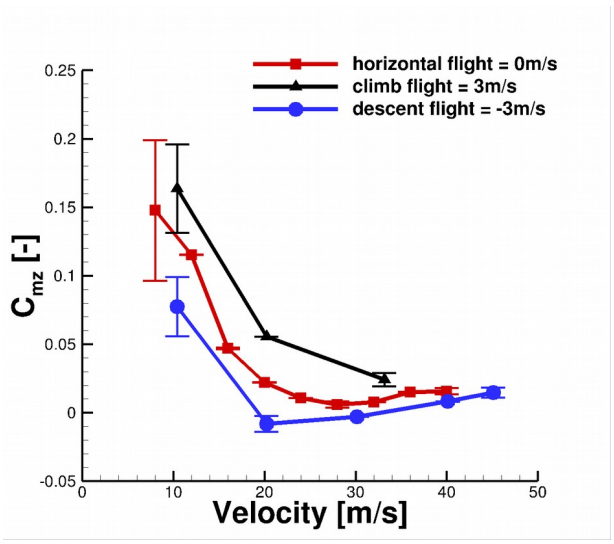

Figure 13: Yawing moment over Velocity

To validate the simulations, the results of the flight test are compared with the results of the flight polar curve. Fig. 14 shows the lift of the elevator for the experiment as well as for the Camrad II simulation and the TAU results. A positive lift value indicates a down force at the horizontal stabilizer of the CoAX 2D and has the same direction as the weight force at the helicopter. It shows a good agreement between the simulations and the experimental data.

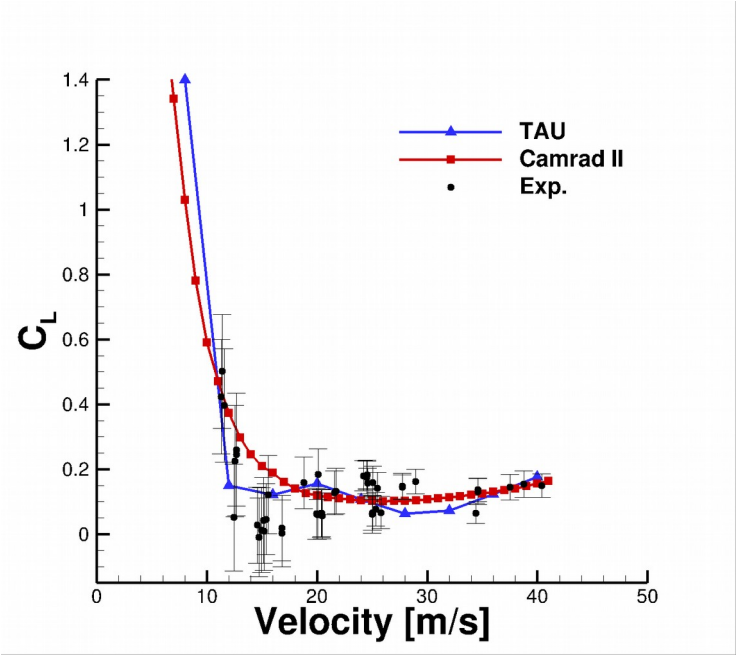

Figure 14: Comparison the force at the horizontal stabilize between measurement data and simulations

Fuselage optimization:

In consultation with the company edm-aerotec, an optimization of the landing gear was decided upon, because in the airworthiness requirement LTF-ULM 2019 [10] the maximum take-off weight was raised from 450kg to 600kg and the current landing gear had to be adapted to the higher weight. Figure 15 shows the current configuration of the landing gear.

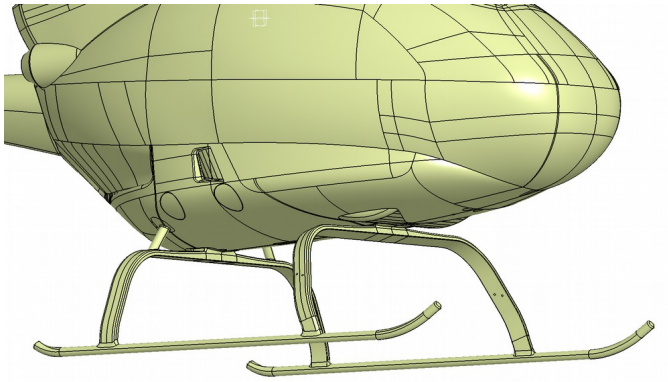

Figure 15: CAD-Geometry from Landing gear

The current landing gear consists of two skid supports which are mounted in the front and rear area of the fuselage and which connect the skids with the fuselage. The skid supports consist of a rectangular profile with rounded corners, which in the case of the CoAX 2D are mounted underneath the fuselage. The skids are made with a circular profile and are bent upwards at the beginning and end. In order to evaluate possible modifications of the landing gear and to determine the potential of a landing gear optimization, a fuselage simulation without landing gear is carried out. The data point is selected with a speed of 32 m/s in horizontal flight from the flight polar and recalculated on a new mesh without landing gear. Care is taken to ensure that the topology of the new and the original mesh are similar in many areas as possible. Due to the missing landing gear in the new mesh, it has 0.9 mio. fewer mesh points than the original mesh.

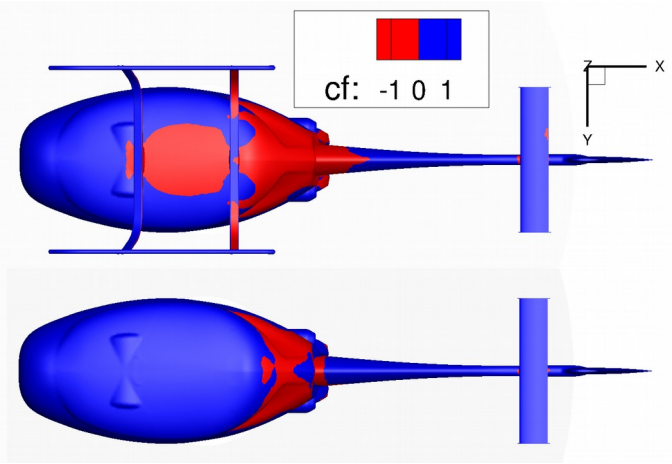

Figure 16: skin friction coefficient between with and without landing gear

Figure 16 shows the dimensionless wall shear stress coefficient. Red areas are negative wall shear stress values and are synonymous with separated flow. The blue areas are positive wall shear stress values and are synonymous with attached flow. By omitting the landing gear, the drag coefficient is reduced by 23.4% for the overall configuration. This is partly due to the reduction of the separation in the lower fuselage area and the omission of the landing gear. In order to exploit as much of this potential, the drag of the landing gear and the interference drag would have to be reduced. It is possible to reduce the interference drag by minimizing the separation between the skid support and the fuselage. This is achieved by moving the connection between the fuselage and the runner into the fuselage interior. In this type of assembly, the skids protrude sideways from the fuselage and do not disturb the flow below the fuselage compared to the previous configuration. A comparable skid support arrangement was successfully demonstrated on the Bluecopter Demonstrator (modified EC135) [11]. Due to the extensive structural changes and the associated redesign of the CoAX 2D, this type of optimisation was not pursued any further. In order to find a optimization, which can be realized with reasonable effort on the CoAX 2D, a change of the skid support profile as well as the distribution of the skid support profiles are changed. Based on the chassis of the Bluecopter, a double ellipse is selected as the profile. The ellipse is adapted so that the height and thus the structural design of the previous rectangular profile is retained.

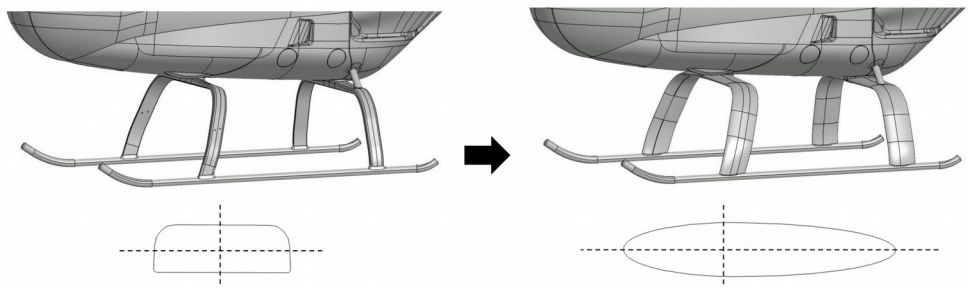

Figure 17: Comparison between new and old geometry

Figure 17 Shows the old skid support profile on the left and the new double elliptical profile on the right. In order to minimize the separation area between the skid beam and the fuselage behind the front skid beam, the front skid beam angle is changed.

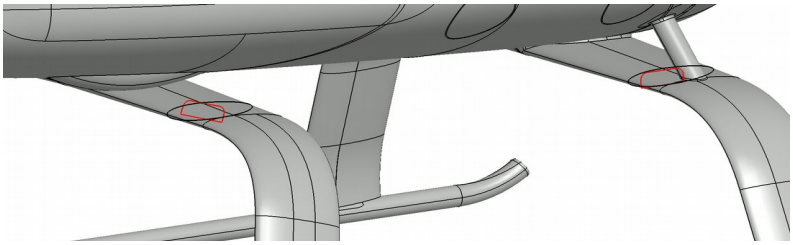

Figure 18: Comparison between the old and new distribution

Picture 18 shows the reduction of the angle of attack in the front area of the skid support in comparison to the old profile. The distribution and the angle of attack of the old profile are taken over from the rear skid support. For the new landing gear, a new calculation mesh is also created and the data point from the flight polar with 32 m/s flight speed in horizontal flight was selected for comparison. Due to the modification of the landing gear, the new computing mesh has 0.3 mio. mesh points more than the previous mesh. As seen in Figure 19, these modifications led to a minimization of the total drag coefficient of 8.29%. On the one hand, this is due to the minimization of the separation in the area between the skid support and the airframe. On the other hand, the separation area behind the skid support is reduced as shown in Figure 20.

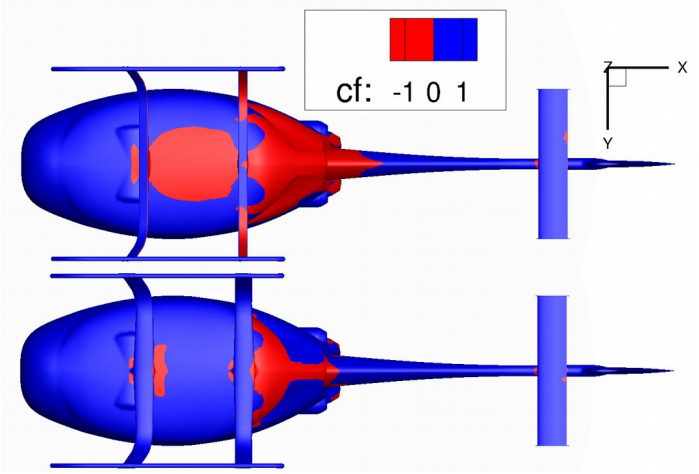

Figure 19: skin friction coefficient between old and new landing gear

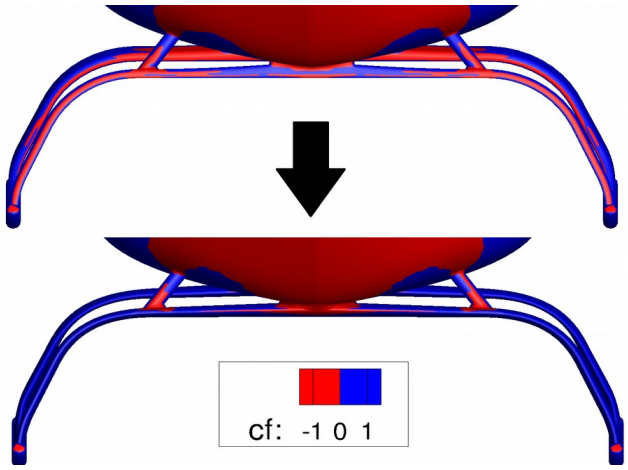

Figure 20:skin friction coefficient between old an new landing gear, rear view

Conclusions

In this paper, the fuselage aerodynamics of the CoAX 2D ultra-light helicopter is examined. In order to get a comprehensive picture, the actual state of the fuselage aerodynamics is evaluated. For this purpose, a variation of the angle of attack and the yaw angle at constant speed is simulated. The simulation is carried out without rotor downwash. In order to consider the influence of the rotor downwind, in the second step the downwash is modelled by means of Actuator Disc. In addition to the angle of attack, the speed is also varied. Comparisons between the simulations and the flight data showed a good agreement. Based on these results, an optimization of the landing gear is carried out. It is shown that the total drag can be minimized by changing the landing gear around 8%.

Acknowledgments

The author of this paper would like to thank Roland Feil from the Technical University of Munich for providing the input data for the Actuator Disc. Further thanks go to the company edm aerotec. Also the author would like to thank Gunther Wilke and Thorsten Schwarz for the help and support in creating this paper.

References

[1] Wayne J. (NASA Ames Research Center), Joshua F. Elmore, Ernest B. Keen, Andrew T. Gallaher and Gerardo F. Nunez (US Army Aviation Development Directorate - AFDD) “Coaxial Compound Helicopter for Confined Urban Operations”

[2] Mikheyev, S., “50 Years Experience, Status, Prospects,” 33rd European Rotorcraft Forum, Plenary Meeting, Kazan, Russia, September 11–14, 2007

[3] www.edm-aerotec.de

[4] Feil, R., Rinker, M., and Hajek, M., “Flight Testing of a Coaxial Ultralight Rotorcraft,” American Helicopter Society 73rd Annual Forum, American Helicopter Soc., Fairfax, VA, 2017, pp. 1–14

[5] R.Feil, D Eble and M. Hajek, "Comprehensive Analysis of a Coaxial Ultralight Rotorcraft and Validation with Full-Scale Flight-Test Data" ,Journal of the American Helicopter Society 63, 042004 (2018)

[6] Fliegermagazin,”Die UL-Helis kommen” 05.2015

[7] D.Schwamborn, T.Gerhold, R.Heinrich “The DLR Tau-code: Recent applications in research and industry”, European Conference on Computational Fluid Dynamics 2006

[8] Raichle A., (2017). “*Flusskonservative Diskretisierung des Wirkscheibenmodells als Unstetigkeitsfläche”*, Dissertation, DLR-Forschungsbericht, DLR-FB-2017-62, 225 S.

[9] Johnson, W., “Technology Drivers in the Development of CAMRAD II,” American Helicopter Society Aeromechanics Specialists’ Conference, San Francisco, CA, January 19–21, 1994.

[10] Bauvorschriften für Ultraleichte Tragschrauber (einmotorig) BUT vom 15.01.2019

[11] Bebesel M., D'Alascio A., Schneider S., Guenther S., Vogel F., Wehle C., Schimke D.,”Bluecopter Demonstrator – an Approach to Eco-efficient Helicopter Design”, 41st European Rotorcraft Forum 2015